Nano Res (2008) 1: 152–157
DOI 10.1007/s12274-008-8013-8
Research Article

High Yield Synthesis and Characterization of the Structural and Magnetic Properties of Crystalline $ErCl_3$ Nanowires in Single-Walled Carbon Nanotube Templates

Ryo Kitaura[1], Daisuke Ogawa[1], keita Kobayashi[1], Takeshi Saito[2,3], Satoshi Ohshima[2], Tetsuya Nakamura[4], Hirofumi Yoshikawa[1], Kunio Awaga[1], and Hisanori Shinohara[1] (✉)

[1] Department of Chemistry and Institute for Advanced Research, Graduate School of Science, Nagoya University, Nagoya 464-8602, Japan
[2] Nanotube Research Center, National Institute of Advanced Industrial Science and Technology, Tsukuba 305-8565, Japan
[3] PRESTO, Japan, Science and Technology Agency, 4-1-8 Honcho kawaguchi, Saitama 332-0012, Japan
[4] Japan Synchrotron Radiation Research Institute, Hyogo 679-5198, Japan

Received: 2 May 2008 / Revised: 13 June 2008 / Accepted: 17 June 2008

ABSTRACT

Crystalline $ErCl_3$ nanowires have been fabricated in single-walled carbon nanotubes (SWCNTs) with high yield (~90%), and the structural and magnetic properties of the resulting $ErCl_3$ nanowires encapsulated in SWCNTs ($ErCl_3$@SWCNTs) characterized. Encapsulation under high temperature and vacuum using high quality SWCNTs results in a high filling-ratio of $ErCl_3$ nanowires in the SWCNTs. The high filling-ratio of $ErCl_3$ nanowires and the use of highly pure SWCNTs with only a small amount of residual Fe catalyst nanoparticles enabled us to observe the magnetic properties of $ErCl_3$@SWCNTs. Structure determination based on simulated annealing calculations and high-resolution transmission electron microscope (HRTEM) image simulations revealed that the structure of the $ErCl_3$ nanowires is unusual with respect to the coordination environment of the Eu^{3+} ions. This work opens up new possibilities to fabricate various metal complex nanowires with high yield and may also be of more general importance in understanding and exploring magnetic properties in low-dimensional magnetic systems.

KEYWORDS

Low-dimensional nanomaterials, carbon nanotubes, magnetic properties, crystal structure, transmission electron microscope

Considerable research efforts have been devoted to the fabrication of low-dimensional nanomaterials because of their specific structures and properties [1–7]. On this basis, we have focused on the development of a facile method for preparing compositionally diverse low-dimensional crystalline materials with diameters in the range of sub-nanometer to several nanometers in order not only to find specific structures resulting from such low-dimensionality, but also to understand the intrinsic properties of low-dimensional nanostructures where quantum size effects play an important role.

One of the most interesting ways to fabricate low-dimensional nanomaterials is to utilize

Address correspondence to noris@nagoya-u.jp

nanometer scale channels as a template, and the one-dimensional nano-channel of single-walled carbon nanotubes (SWCNTs) is suitable for the fabrication and characterization of such novel nanomaterials [8–11]. In fact, metal salts, alloys, and molecules including fullerenes and metallofullerenes have been encapsulated into nano-channels of carbon nanotubes in order to produce low-dimensional arrays of these materials [12–17]. A high filling-ratio and precise structural characterization is crucial in order to understand the properties of low-dimensional nanomaterials fabricated in the nano-channels of SWCNTs. Therefore, in the present study, we have developed an encapsulation method which gives high filling-ratios and a structure determination procedure that is based on a high-resolution electron microscope (HRTEM) image simulation by the multi-slice method and structure construction by the simulated annealing method [18]. These methods have been applied in the synthesis and characterization of $ErCl_3$ nanowires encapsulated in SWCNTs ($ErCl_3$@SWCNTs).

Furthermore, we have successfully measured the magnetic properties of the encapsulated $ErCl_3$ nanowires in $ErCl_3$@SWCNTs by using high quality SWCNTs with only a small amount of Fe impurities. The method can be more generally applied to fabricate various low-dimensional metal complex nanowires and characterize their structural and magnetic properties. This will open up new fields in the science and technology of carbon nanotubes and related low-dimensional nanomaterials.

SWCNTs were synthesized by the so-called extended direct injection pyrolytic synthesis (e-DIPS) [19], and the raw products were annealed at 1200 °C for 24 hours in order to remove any remaining Fe catalyst nanoparticles and amorphous carbon impurities. Figure 1 shows the thermal gravimetric analysis (TGA) trace of the purified SWCNTs. The sharp drop in sample weight at 500 °C and the small amount of residual material (0.87 wt%) indicate the high quality of the purified SWCNTs. Before the encapsulation reaction, the SWCNTs were heated under dry airflow at 600 °C for 30 min in order to remove the end-cap. Open-ended SWCNTs were vacuum-sealed (10^{-7} Torr) in a quartz tube with

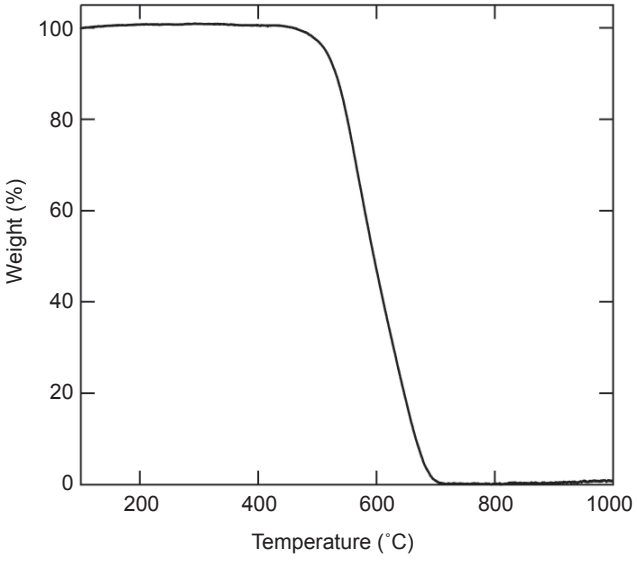

Figure 1 TGA trace of the purified SWCNTs. The sharp drop in sample weight at 500 °C and the small amount of residual material indicate the high quality of the purified SWCNTs

anhydrous $ErCl_3$, and heated at 800 °C for 72 hours. At this temperature, $ErCl_3$ melted and became encapsulated within the core of the SWCNTs. The as-prepared products were washed with MeOH in order to remove any $ErCl_3$ adsorbed on the outer surface of the SWCNTs and then dried at room temperature at 80 °C for 12 hours.

Figure 2 shows a low magnification transmission electron microscope (TEM) image of $ErCl_3$@SWCNTs. Strong contrasts arranged in a regular fashion can be clearly seen, and virtually no $ErCl_3$ attached to the outer surface of the SWCNTs was observed. Fast Fourier transform (FFT) analysis of the image (shown in the inset to Fig. 2) clearly shows lines that originate from the regular array of dark contrasts. We observed many TEM images, and found that SWCNTs without $ErCl_3$ inside were very rarely seen. The estimated filling-ratio from the TEM images is more than 90%. This high filling-ratio was also confirmed by TGA of $ErCl_3$@SWCNTs: the weight percentage of residual material is much larger than that of purified SWCNTs (40.6 wt% and 0.87 wt% for $ErCl_3$@SWCNTs and purified SWCNTs, respectively). The filling-ratio is substantially higher than that previously reported for metal salts encapsulated in SWCNTs. The use of high quality SWCNTs synthesized by e-DIPS, together with carrying out the encapsulation reaction under high vacuum at an

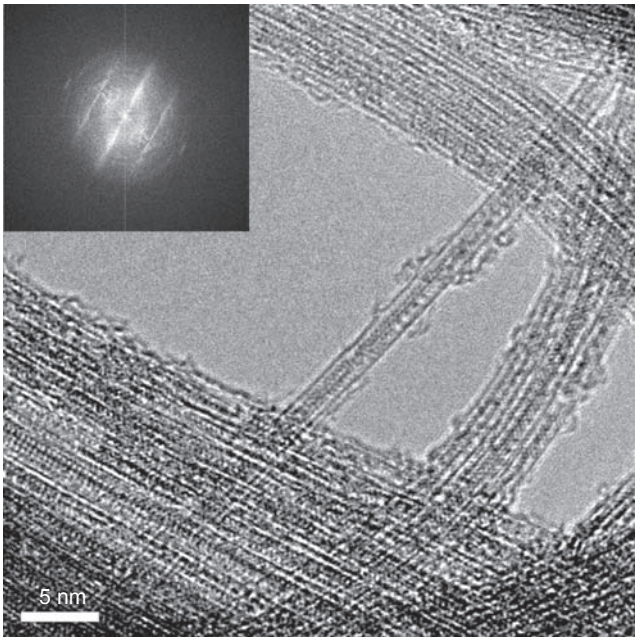

Figure 2 TEM image of a bundle of synthesized $ErCl_3$@SWCNTs. The inset shows the fast Fourier transform (FFT) of the TEM images

optimized temperature are probably the key factors responsible for such high filling-ratios.

Figure 3(a) shows the observed high-resolution TEM (HRTEM) image of $ErCl_3$@SWCNTs. Two columns of dark ellipsoidal spots aligned in a regular fashion are clearly observed in the SWCNT; this regular array indicates the formation of one-dimensional crystalline materials in the SWCNTs. The contrast of dark ellipsoids is stronger than that in SWCNTs themselves, which strongly suggests that the dark ellipsoids originate from species heavier than carbon.

We have also performed direct lattice measurements using the HRTEM image and determined that the unit cell length of the one-dimensional crystal is 4.3 Å. An energy-dispersive X-ray (EDX) spectrum observed in the same area shows strong peaks that can be attributed to Er $M\alpha$, $K\alpha$, $K\beta$ and Cl $K\alpha$ and $K\beta$. The dark spots are not observed in SWCNTs prior to the $ErCl_3$ encapsulation reaction, and the corresponding EDX peaks from Er and Cl are also not observed. Therefore, we can safely conclude that the dark spots originate from encapsulated Er and Cl atoms in $ErCl_3$@SWCNTs.

Based on the observed TEM image, we have constructed a structural model of the nanowires in

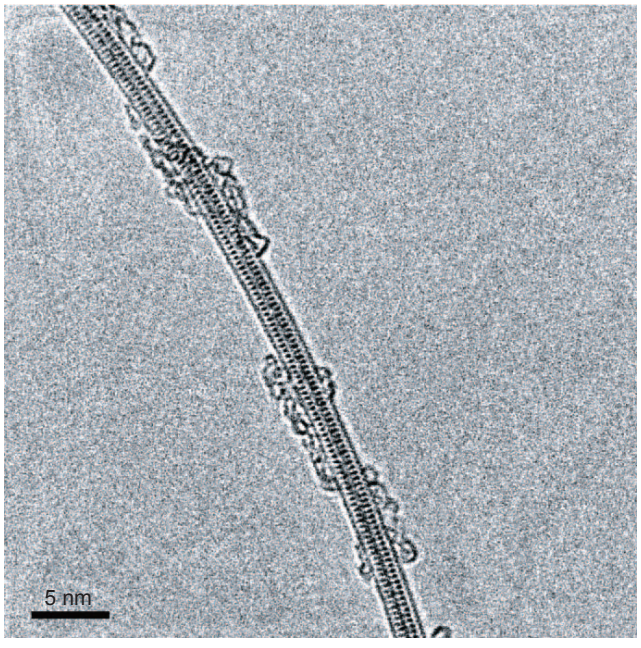

(a)

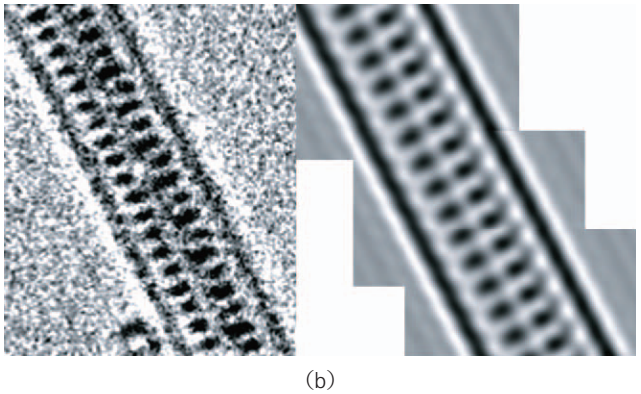

(b)

Figure 3 (a) HRTEM image of $ErCl_3$@SWCNTs. (b) Observed (left) and simulated (right) HRTEM image of $ErCl_3$@SWCNTs

SWCNTs. Simulated annealing calculations have been applied to find the optimum structure with the lowest Coulomb potential energy. In the calculations, the composition ratio of Er/Cl is assumed to be 1:3, and the unit cell length of the one-dimensional crystal is fixed at 4.3 Å. Trivalency of Er ions (i.e., Er^{3+}) was confirmed by X-ray absorption spectrum at the Er M_5 absorption edge, which was identical to that of Er_2O_3 (Fig. 4). Any interaction between the encapsulated species and SWCNTs was not considered, i.e., it is assumed that the SWCNTs act only as a template that restricts the space where Er^{3+} and Cl^- ions are encapsulated.

Figure 5 shows the final constructed possible structure model of $ErCl_3$@SWCNTs. Four columns of

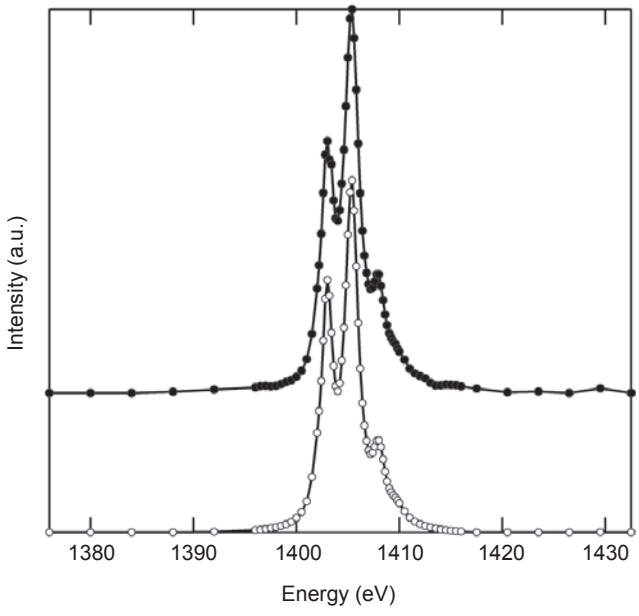

Figure 4 X-ray absorption spectra of $ErCl_3$@SWCNTs and Er_2O_3, confirming the presence of Eu^{3+} in both species. Filled and open circles represent $ErCl_3$@SWCNTs and Er_2O_3, respectively

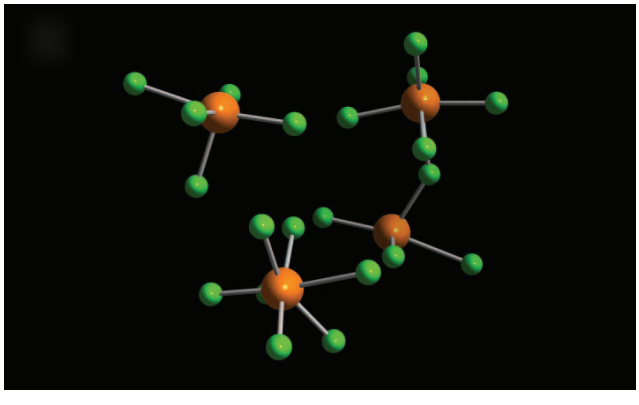

(a)

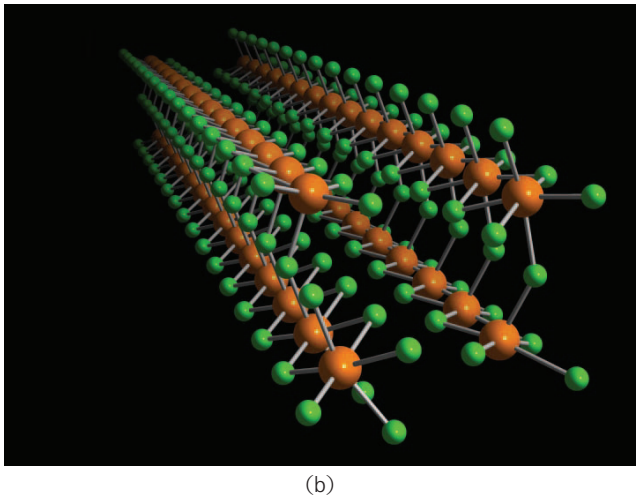

(b)

Figure 5 Possible structure model of the encapsulated crystalline $ErCl_3$ nanowire: (a) the atomic structure of the $ErCl_3$ nanowire in one unit cell; (b) the expanded atomic structure

Er^{3+} ions are aligned along the axis of the SWCNTs. In the structure model, there are two different types of Er^{3+} coordination: (1) distorted square pyramidal coordination (coordination number 5) and (2) distorted octahedral coordination (coordination number 6). Rare earth ions usually have high coordination number ranging from 6 to 10. In particular, Er^{3+} ions in hydrated and anhydrous $ErCl_3$ have coordination numbers of 6 and 8, respectively. The reduced coordination number of Er^{3+} in $ErCl_3$@SWCNTs presumably results from the confinement effect of the nano-channel of SWCNTs: Cl^- ions cannot freely coordinate Er^{3+} ions due to the restricted space of SWCNTs, which leads to the observed low coordination number. The restricted space of SWCNTs is, therefore, well suited to create unusual low-dimensional metal complex nanowires with specific coordination environments.

Using the constructed structure model, HRTEM image simulation by the multi-slice method (at a defocus of 60 nm) has been performed. As illustrated in Fig. 3(b), the simulated HRTEM image reproduces well both the observed dark ellipsoids and their intensities. The possibility of a two or three $ErCl_3$ chain model was excluded by the simulations, because such structure models cannot reproduce the observed intensity ratio between the dark ellipsoids within the SWCNTs and the carbon walls of the SWCNTs. The SWCNTs used in this study possess a relatively large diameter distribution whose mean diameter is around 1.8 nm. The structure of the encapsulated one-dimensional $ErCl_3$ crystal changes according to the diameter of the encapsulating SWCNTs. The above determined crystal structure of $ErCl_3$ was formed in SWCNTs of 1.8 nm diameter, which is the most common type in the sample.

The magnetic susceptibility of $ErCl_3$@SWCNTs has also been measured using SQUID magnetometry. Figure 6 shows the variation with temperature of the magnetic susceptibility of purified empty-SWCNTs and $ErCl_3$@SWCNTs. The magnetization of purified empty-SWCNTs is sufficiently low in the temperature region studied to enable us to observe the magnetization of the encapsulated $ErCl_3$ nanowires in $ErCl_3$@SWCNTs. The high filling-ratio of $ErCl_3$ together with the removal of the Fe catalyst

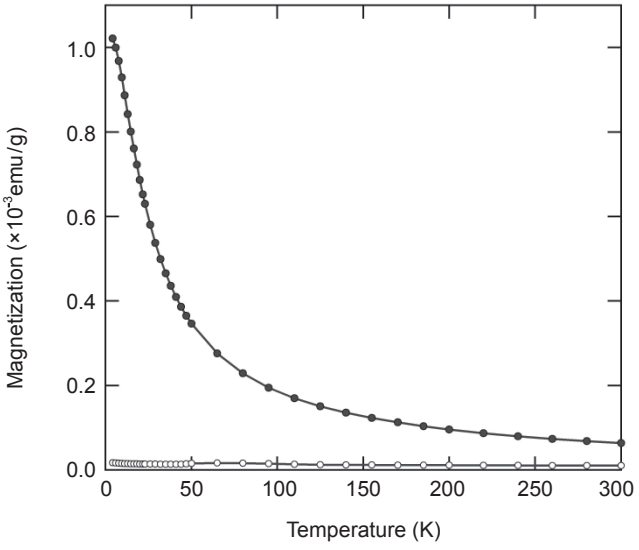

Figure 6 Magnetization of $ErCl_3$@SWCNTs and purified empty-SWCNTs as measured by SQUID magnetometry. Filled and open circles represent magnetization of $ErCl_3$@SWCNTs and purified empty-SWCNTs, respectively

nanoparticles by high-vacuum annealing are the crucial factors in allowing the observation of the magnetization of the encapsulated species.

The magnetization behavior of $ErCl_3$@SWCNTs can be fitted by the Curie–Weiss law, which provides a Curie constant and Weiss temperature. The observed Curie constant corresponds to an effective magnetic moment of 10.7 μ_B, which is consistent with the $4f^{11}$ electronic configuration of Er^{3+} ions. The obtained Weiss temperature was −9.1 K, which indicates a weak antiferromagnetic interaction between Er^{3+} ions. The observed magnetization behavior of $ErCl_3$@SWCNTs was essentially the same as that of bulk anhydrous $ErCl_3$. This is because the spatial spread of the radial wavefunction of the 4f orbitals, which is responsible for the magnetization of Er^{3+} ions, is very small leading to a weak magnetic interaction between neighboring Er^{3+} ions. Therefore, the magnetization of Er^{3+} ions is insensitive to its coordination environment. We can expect a stronger magnetic interaction will be observed by using 3d transition metal complexes; further characterization of the magnetic properties of 3d transition metal complex nanowires formed in SWCNTs is currently under way.

In conclusion, we have successfully fabricated novel low-dimensional crystalline $ErCl_3$ nanowires encapsulated in SWCNTs with high yield (~90%) and characterized their structural and magnetic properties. Encapsulation reactions carried out under high temperature and high vacuum conditions using high quality SWCNTs are necessary in order to obtain such a high filling-ratio synthesis of $ErCl_3$@SWCNTs. A structure determination method based on the simulated annealing method and HRTEM image simulation has been shown to be useful in characterizing the crystal structure of metal complex nanowires formed in SWCNTs. This opens up new possibilities to fabricate various low-dimensional metal complex nanomaterials in SWCNTs with high yield and may also be of more general importance in understanding and exploring magnetic properties in low-dimensional magnetic systems.

Acknowledgements

This work has been supported by the JST CREST Program for novel carbon nanotube materials. The XAS experiments were performed at BL25SU in SPring-8 with the approval of JASRT (Proposal No. 2007B1732).

References

[1] Hu, Y. J.; Xiang, J.; Liang, G. C.; Yan, H.; Lieber, C. M. Sub-100 nanometer channel length Ge/Si nanowire transistors with potential for 2 THz switching speed. *Nano Lett*. **2008**, *8*, 925–930.

[2] Kitaura, R.; Imazu, N.; Kobayashi, K.; Shinohara, H. Fabrication of metal nanowires in carbon nanotubes via versatile nano-template reaction. *Nano Lett*. **2008**, *8*, 693–699.

[3] Ohnishi, H.; Kondo, Y.; Takayanagi, K. Quantized conductance through individual rows of suspended gold atoms. *Nature* **1998**, *395*, 780–783.

[4] Ishii, H.; Kataura, H.; Shiozawa, H.; Yoshioka, H.; Otsubo, H.; Takayama, Y.; Miyahara, T.; Suzuki, S.; Achiba, Y.; Nakatake, M., Narimura, T.; Higashiguchi, M.; Shimada, K.; Namatame, H.; Taniguchi, M. Direct observation of Tomonaga-Luttinger-liquid state in carbon nanotubes at low temperatures. *Nature* **2003**, *426*, 540–544.

[5] Huang, M. H.; Mao, S.; Feick, H.; Yan, H. Q.; Wu, Y. Y.; Kind, H.; Weber, E.; Russo, R.; Yang, P. D. Room-

temperature ultraviolet nanowire nanolasers. *Science* **2001**, *292*, 1897–1899.

[6] Hu, J. T.; Odom, T. W.; Lieber, C. M. Chemistry and physics in one dimension: Synthesis and properties of nanowires and nanotubes. *Acc. Chem. Res.* **1999**, *32*, 435–445.

[7] Hornbaker, D. J.; Kahng, S. J.; Misra, S.; Smith, B. W.; Johnson, A. T.; Mele, E. J.; Luzzi, D. E.; Yazdani, A. Mapping the one-dimensional electronic states of nanotube peapod structures. *Science* **2002**, *295*, 828–831.

[8] Kitaura, R.; Shinohara, H. Carbon-nanotube-based hybrid materials: Nanopeapods. *Chem—Asian J.* **2006**, *1*, 646–655.

[9] Britz, D. A.; Khlobystov, A. N.; Porfyrakis, K.; Ardavan, A.; Briggs, G. A. D. Chemical reactions inside single-walled carbon nano test-tubes. *Chem. Commun.* **2005**, 37–39.

[10] Smith, B. W.; Monthioux, M.; Luzzi, D. E. Encapsulated C60 in carbon nanotubes. *Nature* **1998**, *396*, 323–324.

[11] Bandow, S.; Hiraoka, T.; Yumura, T.; Hirahara, K.; Shinohara, H.; Iijima, S. Raman scattering study on fullerene derived intermediates formed within single-wall carbon nanotube: From peapod to double-wall carbon nanotube. *Chem. Phys. Lett.* **2004**, *384*, 320–325.

[12] Carter, R.; Sloan, J.; Kirkland, A. I.; Meyer, R. R.; Lindan, P. J. D.; Lin, G.; Green, M. L. H.; Vlandas, A.; Hutchison, J. L.; Harding, J. Correlation of structural and electronic properties in a new low-dimensional form of mercury telluride. *Phys. Rev. Lett*. **2006**, *96*, 215501.

[13] Philp, E.; Sloan, J.; Kirkland, A. I.; Meyer, R. R.; Friedrichs, S.; Hutchison, J. L.; Green, M. L. H. An encapsulated helical one-dimensional cobalt iodide nanostructure. *Nat. Mater.* **2003**, *2*, 788–791.

[14] Hirahara, K.; Suenaga, K.; Bandow, S.; Kato, H.; Okazaki, T.; Shinohara, H.; Iijima, S. One-dimensional metallofullerene crystal generated inside single-walled carbon nanotubes. *Phys. Rev. Lett*. **2000**, *85*, 5384–5387.

[15] Takenobu, T.; Takano, T.; Shiraishi, M.; Murakami, Y.; Ata, M.; Kataura, H.; Achiba, Y.; Iwasa, Y. Stable and controlled amphoteric doping by encapsulation of organic molecules inside carbon nanotubes. *Nat. Mater.* **2003**, *2*, 683–688.

[16] Lee, J.; Kim, H.; Kahng, S. J.; Kim, G.; Son, Y. W.; Ihm, J.; Kato, H.; Wang, Z. W.; Okazaki, T.; Shinohara, H.; Kuk, Y. Bandgap modulation of carbon nanotubes by encapsulated metallofullerenes. *Nature* **2002**, *415*, 1005–1008.

[17] Simon, F.; Kuzmany, H.; Rauf, H.; Pichler, T.; Bernardi, J.; Peterlik, H.; Korecz, L.; Fulop, F.; Janossy, A. Low temperature fullerene encapsulation in single wall carbon nanotubes: Synthesis of N@C-60@SWCNT. *Chem. Phys. Lett*. **2004**, *383*, 362–367.

[18] Kirkpatrick, S.; Gelatt, C. D.; Vecchi, M. P. Optimization by simulated annealing. *Science* **1983**, *220*, 671–680.

[19] Saito, T.; Xu, W. C.; Ohshima, S.; Ago, H.; Yumura, M.; Iijima, S. Supramolecular catalysts for the gas-phase synthesis of single-walled carbon nanotubes. *J. Phys. Chem. B* **2006**, *110*, 5849–5853.